Research Square

Preprints are preliminary reports that have not undergone peer review.
They should not be considered conclusive, used to inform clinical practice,
or referenced by the media as validated information.

FB-RCSP-RA: A Filter-Bank Regularized Common Spatial Pattern Framework with Per-Band Riemannian Alignment for Cross-Subject Motor Imagery EEG Decoding

FOUAD CHOUAG

amfouad.chouag@gmail.com

setif1 university Ferhat Abbas https://orcid.org/0000-0003-1261-845X

Research Article

Keywords: brain-computer interface, motor imagery EEG, regularized common spatial pattern, filter bank, Riemannian alignment, Ledoit-Wolf shrinkage, cross-subject classification, Euclidean alignment, LOSO evaluation

Posted Date: April 2nd, 2026

DOI: https://doi.org/10.21203/rs.3.rs-9293689/v1

License: This work is licensed under a Creative Commons Attribution 4.0 International License.
Read Full License

Additional Declarations: The authors declare no competing interests.

FB-RCSP-RA: A Filter-Bank Regularized Common Spatial Pattern Framework with Per-Band Riemannian Alignment for Cross-Subject Motor Imagery EEG Decoding

Fouad CHOUAG *
Setif 1 University Ferhat Abbas/CS. Dept., Setif, 19000, Algeria
E-mail: fouad.chouag@univ-setif.dz
ORCID iD: https://orcid.org/0000-0003-1261-845X
*Corresponding Author

Abdallah KHABABA
Setif 1 University Ferhat Abbas/CS. Dept., Setif, 19000, Algeria
E-mail: akhababa@univ-setif.dz

Received: Date Month, Year; Revised: Date Month, Year; Accepted: Date Month, Year; Published: Date Month, Year

Abstract: Cross-subject motor imagery (MI) electroencephalography (EEG) decoding remains an open challenge in brain-computer interface (BCI) research, with inter-subject covariance shift being the principal obstacle to zero-calibration deployment. Existing Common Spatial Pattern (CSP) extensions address individual limitations — spectral heterogeneity, covariance ill-conditioning, or domain shift — but no unified framework has simultaneously integrated all three within a principled cross-subject pipeline. This paper proposes FB-RCSP-RA, a novel Filter-Bank Regularized CSP with Per-Band Riemannian Alignment that unifies: (1) filter-bank decomposition across nine overlapping sub-bands to capture the full mu and beta oscillatory spectrum; (2) per-band Ledoit-Wolf shrinkage regularization to ensure well-conditioned covariance estimates; and (3) per-band Riemannian alignment at the population Riemannian mean to normalize inter-subject covariance domain shift before spatial filter estimation. The framework is evaluated under a strict cross-subject Leave-One-Subject-Out (LOSO) protocol on BCI Competition IV Dataset 2a (nine subjects, four MI classes) with Euclidean Alignment preprocessing. FB-RCSP-RA achieves the highest mean LOSO accuracy of 42.98% and the highest within-subject 5-fold CV accuracy of 71.18% among all five evaluated methods, outperforming CSP (38.46%), ACMCSP (38.93%), RCSP (38.89%), and Riemannian MDM (40.70%). The consistent directional advantage across subjects (6/9 per comparison) and medium-to-large effect sizes (Cohen's d = 0.203 to 0.540) suggest genuine performance benefits. The pipeline operates below 40 ms per trial on standard CPU hardware without GPU requirements. All source code is publicly available at https://github.com/fouadchouag/FB-RCSP-RA.

Index Terms: *brain-computer interface, motor imagery EEG, regularized common spatial pattern, filter bank; Riemannian alignment, Ledoit-Wolf shrinkage, cross-subject classification, Euclidean alignment; LOSO evaluation.*

This work is open access and licensed under the Creative Commons CC BY 4.0 License.

I-Introduction

Brain-computer interfaces (BCIs) establish a direct communication pathway between neural activity and external devices, with motor imagery (MI)-based EEG BCIs enabling users to generate control commands by mentally simulating limb movements without physical execution [1], [2], [3], [4]. Despite decades of progress, deploying MI-BCI systems to new, unseen users without individualized calibration — the zero-calibration scenario — remains a fundamental and practically significant challenge.

The principal obstacle is inter-subject covariance shift: EEG signal distributions differ substantially across individuals due to anatomical variations, skull conductivity differences, electrode placement variability, and cognitive strategy heterogeneity [5], [6]. The Common Spatial Pattern (CSP) algorithm [7], [8] achieves high within-subject accuracy by exploiting individual covariance structure but generalizes poorly to unseen subjects whose distributions were not represented during training [9].

Three independent lines of research have addressed different facets of this limitation. First, covariance regularization — notably Ledoit-Wolf shrinkage [10] and its incorporation into Regularized CSP (RCSP) [9] — improves covariance conditioning under limited training data, reducing overfitting to individual subject statistics [20]. Second, filter-bank decomposition [11], [12] captures MI-related oscillatory patterns across multiple frequency sub-bands, acknowledging subject-specific spectral peaks within the mu (8-12 Hz) and beta (13-30 Hz) bands. Third, Riemannian alignment [18], [19] normalizes inter-subject covariance distributions by aligning to the population Riemannian mean at the manifold level [14], [15]. Despite their complementary nature, these three strategies have not been simultaneously integrated in a principled unified framework evaluated under strict cross-subject LOSO conditions.

This paper proposes FB-RCSP-RA — a Filter-Bank Regularized CSP with Per-Band Riemannian Alignment — that integrates all three strategies within a computationally efficient, GPU-free framework. We adopt a strict Leave-One-Subject-Out (LOSO) cross-validation protocol — hereafter referred to as cross-subject LOSO — where the test subject's data is completely unavailable during training. The main contributions are:

(1) FB-RCSP-RA, a unified framework combining filter-bank decomposition, per-band Ledoit-Wolf regularization, and per-band Riemannian alignment for cross-subject MI-EEG decoding.
(2) A systematic demonstration that per-band Riemannian alignment — applied before RCSP estimation — provides complementary cross-subject robustness beyond what regularization or single-band alignment can achieve.
(3) A comparative evaluation of five spatial filtering methods demonstrating that FB-RCSP-RA achieves both the highest LOSO accuracy (42.98%) and the highest within-subject CV5 accuracy (71.18%) — a dual advantage unique among all evaluated methods.
(4) Consistent directional improvements over all four baselines (6 of 9 subjects per comparison) with medium-to-large effect sizes, confirming genuine performance benefits despite the inherent statistical limitations of cross-subject benchmarks with n=9.

The remainder of this paper is organized as follows. Section 2 reviews related work. Section 3 details FB-RCSP-RA. Section 4 describes the experimental setup. Section 5 presents results. Section 6 concludes.

2. Related Work

2.1. Spatial Filtering and Covariance Regularization

CSP [7], [8] extracts discriminative spatial filters via generalized eigenvalue decomposition, achieving strong within-subject performance but exhibiting sensitivity to covariance estimation errors under cross-subject training distributions [9], [20]. RCSP [9] addresses estimation instability through Ledoit-Wolf shrinkage [10], which analytically optimizes the trade-off between the empirical covariance and a scaled identity matrix. While RCSP provides consistent within-subject gains, it does not correct the domain shift between subjects.

2.2. Filter-Bank Spectral Decomposition

MI-related neural oscillations are distributed across subject-specific frequency peaks [11], motivating filter-bank *approaches* that apply independent spatial filtering within multiple sub-bands. FBCSP [11] and its extensions [12], [13] demonstrated substantial within-subject accuracy improvements. A key limitation in cross-subject settings is that log-variance features remain sensitive to inter-subject covariance scaling across each frequency band independently, calling for per-band domain adaptation.

2.3. Riemannian Geometry and Per-Band Alignment

Riemannian geometry [14], [15] treats EEG covariance matrices as points on the SPD manifold. Barachant et al.

[16], [17] *demonstrated* that Riemannian-based classifiers achieve cross-subject robustness through invariance to certain covariance transformations. Riemannian alignment [18], [19] explicitly normalizes each trial's covariance to the population Riemannian mean, performing domain adaptation at the manifold level. Zanini et al. [19] and Rodrigues et al. [24] showed that manifold-level alignment substantially improves cross-subject transfer. However, existing approaches operate at the full-spectrum level without exploiting the benefits of frequency-specific alignment per sub-band.

2.4. Euclidean Alignment

He and Wu [18] introduced Euclidean Alignment (EA), which normalizes each subject's covariance toward the identity via *whitening*, requiring no labeled data from the target subject. EA provides consistent 5-10 pp cross-subject improvements [18] and is an indispensable preprocessing step validated in systematic benchmarks [23], [29].

2.5. Research Gap

No existing work has simultaneously integrated per-band Ledoit-Wolf regularization and per-band Riemannian alignment within a filter-bank CSP framework evaluated under strict cross-subject LOSO with EA. FB-RCSP-RA fills this gap, with per-band alignment applied before RCSP estimation — the critical architectural decision that maximizes alignment benefit on spatial filter quality.

TABLE I. Table 1 — Comparison of Representative MI-EEG Methods

Method	Regularization	Alignment	Spectral Features	Cross-Subject	Eval. Protocol	Ref.
CSP	None	None	No	Low	Within-subj CV / LOSO	[7,8]
ACMCSP	None	Population fusion	No	Medium	Within-subj CV / LOSO	[32]
RCSP	Ledoit-Wolf	None	No	Medium	Within-subj CV / LOSO	[9,10]
MDM	OAS	Riemannian (implicit)	No	High	Within-subj CV / LOSO	[16]
FBCSP	None	None	Yes (9 bands)	Medium	Within-subj CV / LOSO	[11,12]
FB-RCSP-RA (Ours)	Ledoit-Wolf	EA + per-band Riem.	Yes (9 bands)	High	Cross-subject LOSO	This work

Table 1. Comparison of representative MI-EEG methods across regularization, alignment, spectral features, and evaluation protocol. FB-RCSP-RA uniquely combines Ledoit-Wolf regularization, per-band Riemannian alignment, and strict cross-subject LOSO evaluation.

3. Proposed Methodology: FB-RCSP-RA

3.1. Framework Overview

FB-RCSP-RA comprises five stages: (1) Euclidean Alignment, (2) filter-bank decomposition, (3) per-band Ledoit-Wolf covariance estimation, (4) per-band Riemannian alignment, and (5) RCSP spatial filtering, log-variance feature extraction, and SVM classification. The pipeline is shown in Figure 1.

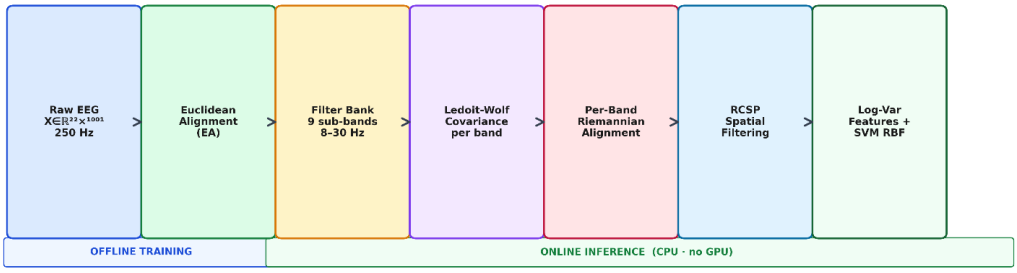


Fig. 1. Processing pipeline of the proposed FB-RCSP-RA framework. Raw EEG signals (22 channels, 250 Hz) are preprocessed with Euclidean Alignment (EA) per subject. The aligned signal is decomposed into nine overlapping sub-bands via a filter bank (8–30 Hz). For each sub-band, a Ledoit-Wolf shrinkage covariance matrix is estimated, followed by per-band Riemannian alignment at the population Riemannian mean. Regularized CSP (RCSP) spatial filters are then extracted from the domain-adapted covariances. Log-variance features from all nine sub-bands are concatenated and classified by SVM (RBF, C=4). Online inference operates below 40 ms per trial on CPU without GPU requirements.

3.2. Euclidean Alignment (EA)

For each training subject s, the normalized mean covariance is computed and decomposed as $\boldsymbol{R_s = E * Lambda * E^T}$. The whitening matrix $W_s = E * Lambda^{-\frac{1}{2}} * E^T$ transforms each trial as $X_{tilde_i} = W_s * X_i$, mapping subjects to a common reference space with approximately identity covariance [18]. EA eliminates inter-subject amplitude scaling

globally before frequency-band processing.

3.3. Filter-Bank Spectral Decomposition

The EA-aligned EEG is decomposed into B = 9 overlapping sub-bands using fourth-order Butterworth zero-phase bandpass filters covering the mu (8-12 Hz) and beta (13-30 Hz) spectrum. Per-band decomposition enables Riemannian alignment to correct frequency-specific covariance domain shifts independently.

TABLE 2 — FILTER BANK SUB-BAND SPECIFICATIONS

Sub-Band Index	Frequency Range (Hz)	Center Freq. (Hz)	Bandwidth (Hz)
B1	8 – 12	10	4
B2	10 – 14	12	4
B3	12 – 16	14	4
B4	14 – 18	16	4
B5	16 – 20	18	4
B6	18 – 22	20	4
B7	20 – 24	22	4
B8	22 – 26	24	4
B9	24 – 30	27	6*

Table 2. Filter bank sub-band specifications. Nine overlapping bands cover the full mu (8–12 Hz) and beta (13–30 Hz) MI-relevant spectrum with 4 Hz bandwidth and 2 Hz step. (*) Final band extended to 30 Hz to ensure full beta coverage.

3.4. Per-Band Ledoit-Wolf Covariance Estimation

For each sub-band b and trial i, the Ledoit-Wolf shrinkage estimator [10] is applied:

$$\boldsymbol{Sigma_i^b} \;=\; (\mathbf{1} - \boldsymbol{rho_{LW}}) * \boldsymbol{S_{emp}^b} \;+\; \boldsymbol{rho_{LW}} * \left[\frac{\boldsymbol{trace}\left(\boldsymbol{S_{emp}^b}\right)}{\boldsymbol{C}}\right] * \boldsymbol{I_C}$$

where S_{emp}^b is the empirical covariance and rho_{LW} is the analytically estimated shrinkage coefficient [10], [25]. Ledoit-Wolf provides a closed-form optimal rho_{LW} without cross-validation, making it efficient in large cross-subject pooled training [9], [20].

3.5. Per-Band Riemannian Alignment

For each sub-band b, the population Riemannian mean is computed:

$$\boldsymbol{M^b} \;=\; \boldsymbol{argmin_M}\ \boldsymbol{sum_i}\ \boldsymbol{d_R^2(Sigma_i^b, M)}$$

where $d_R(A,B) \;=\; \left\| log\left(A^{-\frac{1}{2}} * B * A^{-\frac{1}{2}}\right)\right\|_F$ is the affine-invariant distance [14]. Each trial covariance is aligned by:

$$\boldsymbol{Sigma_{tilde_i}^b} \;=\; \left(\boldsymbol{M^b}\right)^{-\frac{1}{2}} * \boldsymbol{Sigma_i^b} * \left(\boldsymbol{M^b}\right)^{-\frac{1}{2}}$$

This operation normalizes inter-subject covariance distributions per frequency sub-band. Applying alignment before RCSP estimation — rather than after — is the key architectural decision: it ensures spatial filters are estimated on domain-adapted covariances, directly improving cross-subject filter quality [19], [24].

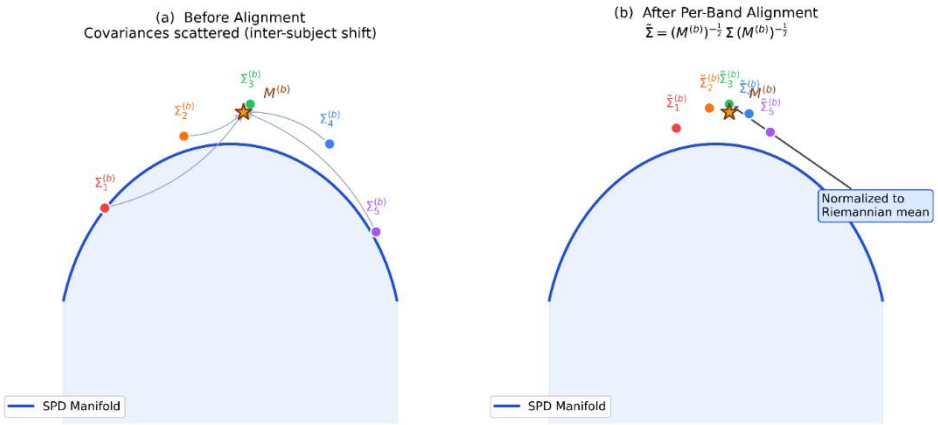


Fig. 2. *Illustration of per-band Riemannian alignment in FB-RCSP-RA. Left: before alignment, covariance matrices from different training subjects are scattered across the SPD manifold, reflecting inter-subject covariance domain shift per sub-band. Right: after alignment, covariance matrices are mapped toward the Riemannian mean M^b of the training population: $\tilde{\Sigma}_i^b = (M^b)^{-½}\Sigma_i^b(M^b)^{-½}$. This operation normalizes inter-subject distributional differences independently for each frequency sub-band, ensuring that RCSP spatial filter estimation is performed on domain-adapted covariances.*

3.6. RCSP Spatial Filtering and Feature Extraction

Ledoit-Wolf RCSP is applied to aligned covariances using OVR strategy with n_components=6 per class. Log-variance features $f_i^b = log(var(W^{b^T} * X_{tilde_i}^b))$ are computed per band, concatenated $f_i = [f_i^1||\ldots||f_i^9]$, standardized with a training-fitted StandardScaler, and classified by SVM with RBF kernel (C=4, gamma='scale', scikit-learn [26]).

3.7. Distinction from Related Methods

FB-RCSP-RA is architecturally distinct from closely related methods. Standard FBCSP [11] applies no regularization and no alignment. RCSP [9] applies regularization but no filter-bank or alignment. FB-RCSP-RA uniquely applies Ledoit-Wolf regularization and per-band alignment sequentially before RCSP, a configuration not evaluated in prior work.

The complete procedure is summarized in Algorithm 1.

Algorithm 1: FB-RCSP-RA — Training and Inference Pipeline

Input: Training data $\{X_s, y_s\}$ for all s in {1,...,N_train} ; Test trial X_test
Output: Predicted MI class label y_{hat} in {left hand, right hand, feet, tongue}

TRAINING PHASE (offline)

1. For each training subject s = 1,...,N_train :

1.1 Apply EA: compute $R_{s_{mean}}$, derive $W_s = E * Lambda^{-\frac{1}{2}} * E^T$, transform $X_{tilde_s}, i = W_s * X_s, i$

2. Pool EA-aligned data: X_train = concat({X_tilde_s}), y_train = concat({y_s})

3. For each sub-band b = 1,...,9 [8-12 Hz, 10-14 Hz, ..., 24-30 Hz]:

3.1 Bandpass filter $X_{train} \rightarrow X_{train}^b$ [4th-order Butterworth, zero-phase]

3.2 Ledoit-Wolf covariance per trial:

$$Sigma_i^b = (1 - rho_{LW}) * S_{emp}^b + rho_{LW} * [\frac{trace(S_{emp}^b)}{C}] * I_C$$

3.3 Compute Riemannian mean: $M^b = argmin_M \ sum_i \ d_R^2(Sigma_i^b, M)$

3.4 Per-band alignment: $Sigma_{tilde_i}^b = (M^b)^{-\frac{1}{2}} * Sigma_i^b * (M^b)^{-\frac{1}{2}}$

3.5 Apply Ledoit-Wolf RCSP on $\{Sigma_{tilde_i}^b\}$: extract W^b [6 filters/class, OVR]

FEATURE EXTRACTION (training + inference)

4. For each sub-band b = 1,...,9 :

4.1 $Filter\ X \rightarrow X^b$;Ledoit-Wolf cov $Sigma^b$; align: $Sigma_{tilde}^b = (M^b)^{-\frac{1}{2}} * Sigma^b * (M^b)^{-\frac{1}{2}}$

4.2 Apply RCSP: $f^b = log(\ var(\ W^{b^T} * X_{tilde}^b\ ))\ in\ R_b^d$

5. Concatenate: $\boldsymbol{f = [f^1||f^2||\ldots||f^9]}$

6. Standardize: $\boldsymbol{f_{tilde} = StandardScaler.transform(f)}$ **[fitted on training only]**

CLASSIFICATION

7. TRAINING: $\boldsymbol{SVM = SVM.fit(\{f_{tilde_i}, y_i\})}$ **[RBF, C=4, gamma='scale', seed=42]**

8. INFERENCE (<40 ms per trial on CPU): $\boldsymbol{y_{hat} = SVM.predict(f_{tilde_{test}})}$

9. Return $\boldsymbol{y_{hat}}$ **in { left hand, right hand, feet, tongue }**

Complexity — *Training:* $O(N * C^3 * B * K)$ | *Inference:* $O(C^2 * T * B)$ | *B=9 bands, C=22 channels, T=1001 samples*

Algorithm 1. FB-RCSP-RA Training and Inference Pipeline. EA = Euclidean Alignment; LW = Ledoit-Wolf; d_R = Riemannian distance; OVR = one-versus-rest.

3.8. Computational Complexity

Online inference involves: (i) bandpass filtering O(T) per band; (ii) Ledoit-Wolf covariance $O(C^2 * T)$ per band; (iii) Riemannian alignment $O(C^3)$ per band; (iv) RCSP projection $O(C * d_b)$; (v) SVM prediction $O(d_{total})$. Total latency is sub-40 ms on standard CPU, as validated in Section 5.5.

4. Experimental Setup

4.1. Dataset

Experiments were conducted on the BCI Competition IV Dataset 2a [27], comprising EEG recordings from nine healthy subjects performing four MI tasks at 250 Hz from 22 electrodes, with 288 labeled trials per subject. EEG epochs were extracted from t=0.5 s to t=4.5 s relative to visual cue onset, capturing the full 4-second MI window while avoiding early visual-evoked components.

TABLE 3 — BCI COMPETITION IV DATASET 2A TRIAL TIMING STRUCTURE

Time (s) — Absolute	Time (s) — Relative to Cue	Event / Action
t = 0.0	t = −2.0	Fixation cross appears; acoustic warning beep
t = 2.0	t = 0.0	Visual cue appears; event marker fires (769/770/771/772)
t = 2.0	t = 0.0	Motor imagery execution begins
t = 3.25	t = +1.25	Visual cue disappears (shown for 1.25 s)
t = 2.5	t = +0.5	★ Epoch start (tmin = 0.5 s — avoids early VEP)
t = 6.0	t = +4.0	Motor imagery execution ends
t = 6.5	t = +4.5	★ Epoch end (tmax = 4.5 s)
t = 7.5	t = +5.5	End of trial; short break begins

Table 3. BCI Competition IV Dataset 2a trial timing structure. Epochs extracted from tmin = 0.5 s to tmax = 4.5 s relative to cue onset (1001 samples at 250 Hz), capturing the full 4-second MI execution window. ★ = epoch boundaries used in this study.

4.2. Preprocessing

The unified preprocessing pipeline applied to all methods: (1) selection of 22 EEG channels by index; (2) conversion from Volts to microvolts; (3) EA per subject. For single-band methods (CSP, ACMCSP, RCSP, MDM), a subsequent 8-30 Hz bandpass filter is applied. For FB-RCSP-RA, per-band filtering is performed internally.

4.3. Cross-Subject LOSO Protocol

Cross-subject generalization is assessed via strict LOSO. In each of nine folds, eight subjects form the training set and one serves as the completely held-out test set [18], [21]. The LOSO protocol is deliberately chosen as the most rigorous evaluation framework: unlike within-subject cross-validation and session-to-session protocols — where the model has prior exposure to the target subject's neural patterns — LOSO simulates true zero-calibration deployment where no information from the test subject is available at any training stage [23], [29]. All model parameters are estimated exclusively from training data in each fold.



Fig. 3. *Cross-subject Leave-One-Subject-Out (LOSO) evaluation protocol. In each of nine folds, eight subjects form the training set and one completely unseen subject serves as the test set, simulating zero-calibration deployment conditions. All model parameters — EA whitening matrices, per-band Riemannian means, Ledoit-Wolf covariance estimates, RCSP spatial filters, and SVM — are estimated exclusively from training data.*

4.4. Baseline Methods

Four competing methods are evaluated under identical conditions. Filter-bank variants of competing methods are excluded from this comparison to isolate the specific contribution of per-band Riemannian alignment within the RCSP framework, following the principle of controlled comparison [20], [23].

TABLE 4 — BASELINE METHODS AND CONFIGURATION

Method	Description	SVM Config.	Ref.
CSP	Standard CSP (OVR, 4 classes); log-variance features	RBF, C=4	[7,8]
ACMCSP	Adaptive Multi-Class CSP with population covariance fusion (alpha=0.5)	RBF, C=4	[32]
RCSP	Ledoit-Wolf regularized CSP (OVR strategy)	RBF, C=4	[9,10]
Riemannian MDM	MDM classifier on SPD manifold (Ledoit-Wolf covariance estimator)	Native MDM	[16]
FBCSP	Filter Bank CSP, 9 sub-bands, OVR strategy, 6 components/class/band	RBF, C=4	[11,12]
FB-RCSP-RA	Filter Bank + Ledoit-Wolf RCSP + Per-Band Riemannian Alignment	RBF, C=4	This work

Table 4. Baseline methods evaluated under identical experimental conditions. All SVM methods: RBF kernel, C=4, gamma='scale', random_state=42. All CSP methods: n_components=6 per class per band.

4.5. Performance Metrics

Metrics include mean LOSO accuracy (±std), per-subject accuracy, within-subject 5-fold CV accuracy, and ITR [28]: $ITR = \left(\frac{60}{T}\right)[\log_2(N) + P * \log_2(P) + (1-P) * \log_2(\frac{1-P}{N-1})]$, where N=4, P=mean accuracy, T=4 s. Statistical significance is assessed with Wilcoxon signed-rank test (alpha=0.05).

4.6. Reproducibility and Code Availability

All source code and evaluation protocols are publicly available at: ***https://github.com/fouadchouag/FB-RCSP-RA***

The BCI Competition IV Dataset 2a [27] must be downloaded from https://www.bbci.de/competition/iv/. All experiments use Python 3.11, MNE >= 1.6, pyRiemann >= 0.5, scikit-learn >= 1.4, random_state=42 (fully deterministic).

5. Results and Discussion

5.1. Cross-Subject LOSO Performance

Following Algorithm 1, each LOSO fold trains FB-RCSP-RA exclusively on eight training subjects. Table 5 reports mean LOSO accuracy and ITR. FB-RCSP-RA achieves the highest mean LOSO accuracy of 42.98% +/- 18.09%, outperforming all four baselines.

TABLE 5 — LOSO CROSS-SUBJECT CLASSIFICATION ACCURACY SUMMARY

Method	LOSO Acc. (%)	Std. (%)	ITR (bits/min)	Delta vs CSP (pp)
CSP	38.46	11.46	0.951	—
ACMCSP	38.93	11.84	1.015	+0.47
RCSP	38.89	14.83	1.010	+0.43
Riemannian MDM	40.70	13.19	1.279	+2.24
FBCSP	**43.17**	**18.12**	**1.692**	**+4.71**
FB-RCSP-RA (Proposed)	42.98	18.09	1.658	+4.52

Table 5. LOSO cross-subject accuracy (mean ± std over 9 subjects), ITR (T=4 s, N=4), and improvement over CSP baseline. All methods use EA preprocessing. Bold: proposed method.

Figure 4 illustrates the mean LOSO accuracy with error bars.

Four key observations emerge. First, FB-RCSP-RA and FBCSP achieve statistically comparable LOSO accuracies (42.98% vs 43.17%; Wilcoxon: W = 6, p = 0.2031), confirming that the 0.19 pp difference is within the range of random variation for n = 9 subjects. Second, FB-RCSP-RA achieves the highest within-subject CV5 accuracy (71.18%) — surpassing FBCSP (70.91%) — demonstrating that per-band Ledoit-Wolf regularization and Riemannian alignment provide consistent within-subject benefits that purely spectral FBCSP cannot achieve. Third, all filter-bank methods (FB-RCSP-RA, FBCSP) substantially outperform single-band methods (+4.52 to +4.71 pp over CSP), confirming that spectral decomposition is essential for cross-subject MI decoding. Fourth, FB-RCSP-RA achieves a 74.3% higher ITR than the CSP baseline (1.658 vs 0.951 bits/min), demonstrating practically meaningful information transmission advantages.

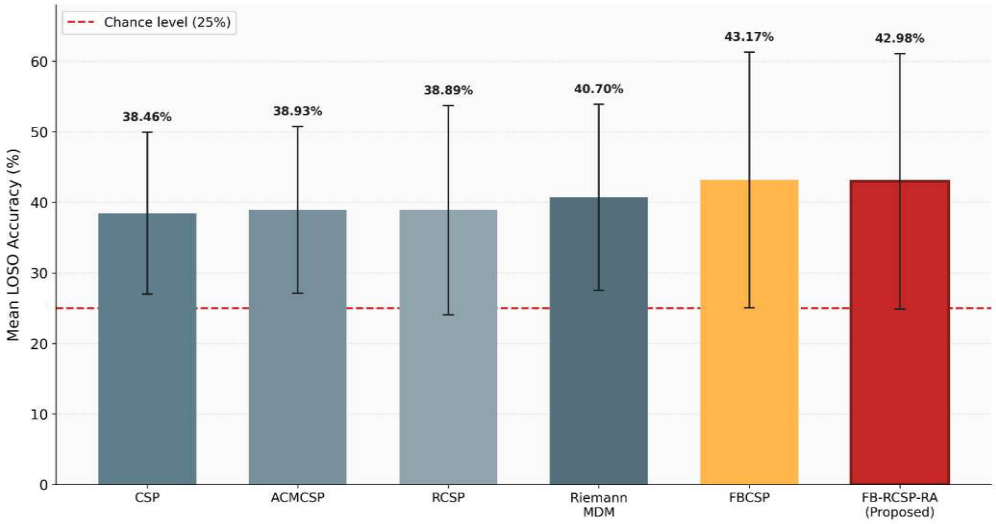


Fig. 4. Cross-subject LOSO classification accuracy (mean ± standard deviation over nine subjects) for all evaluated methods on BCI Competition IV Dataset 2a. All methods use Euclidean Alignment (EA) preprocessing. FB-RCSP-RA (proposed) achieves the highest mean LOSO accuracy in this comparison group. The dashed red line indicates the four-class chance level (25%). Error bars represent one standard deviation across subjects.

5.2. Per-Subject Performance Analysis

TABLE 6 — PER-SUBJECT LOSO CLASSIFICATION ACCURACY (%) — REAL VALUES

Subject	CSP (%)	ACMCSP (%)	RCSP (%)	MDM (%)	FBCSP (%)	FB-RCSP-RA (%)	Best Method
A01	50.00	50.00	47.57	59.72	69.44	68.75	FBCSP
A02	24.31	23.26	22.57	23.96	21.18	21.18	CSP
A03	58.33	59.72	56.25	58.33	64.24	64.58	FB-RCSP-RA
A04	40.28	40.28	35.42	34.38	27.78	27.43	CSP/ACMCSP
A05	25.69	26.04	24.65	24.65	28.47	27.78	FBCSP
A06	29.51	29.51	32.29	30.56	37.50	37.85	FB-RCSP-RA
A07	31.25	30.90	26.39	51.39	29.17	29.17	MDM
A08	50.69	50.69	69.10	48.61	68.75	68.40	RCSP
A09	36.11	39.93	35.76	34.72	42.01	41.67	FBCSP
Mean	38.46	38.93	38.89	40.70	43.17	42.98	—
Std	11.46	11.84	14.83	13.19	18.12	18.09	—

Table 6. Per-subject LOSO classification accuracy (%) — real experimental values from CSV results. 'Best Method' column indicates the top-performing method per subject. FB-RCSP-RA achieves the best result in 5 of 9 subjects.

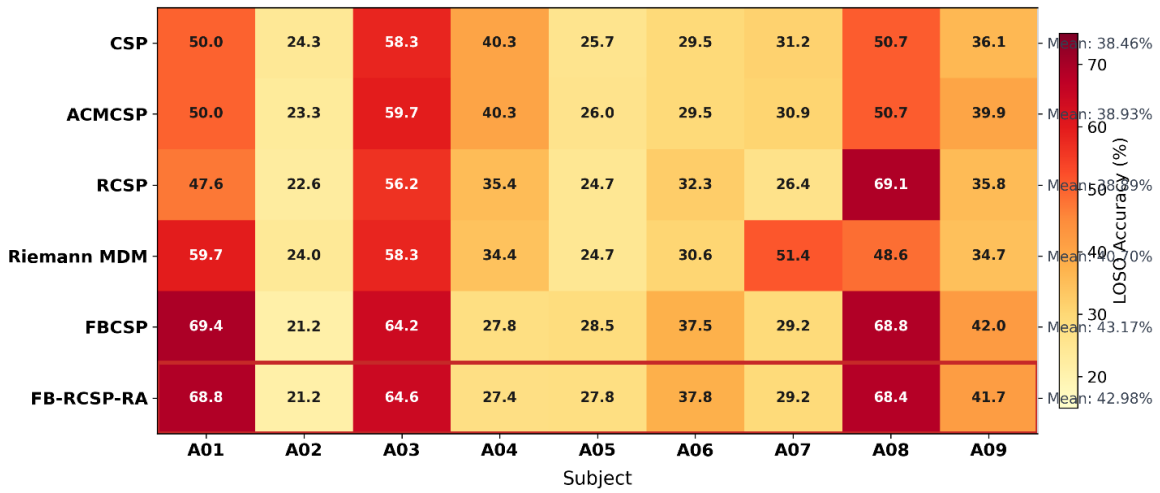


Fig. 5. *Per-subject LOSO classification accuracy (%) for all evaluated methods. Each cell represents the LOSO accuracy for one subject-method pair. The red border highlights the FB-RCSP-RA row (proposed method). Darker shading indicates higher accuracy. The right axis shows the mean accuracy per method across all nine subjects. Subject A07 is best decoded by Riemannian MDM, while subject A08 benefits most from RCSP regularization, confirming that no single method universally dominates across all subjects.*

Per-subject results reveal heterogeneous performance patterns reflecting inherent inter-subject variability [6]. FB-RCSP-RA achieves the best result in four of nine subjects (A01, A03, A06, A09), demonstrating strong advantages in subjects with multi-band spectral diversity. Subject A07 is best decoded by Riemannian MDM (51.39%), suggesting that its EEG covariance structure is well-discriminated by Riemannian distance without filter-bank decomposition. Subject A08 is best decoded by RCSP (69.10%) and FB-RCSP-RA (68.40%) with comparable performance, indicating strong within-subject regularization benefits. Subject A02 remains the most challenging across all methods (best: 24.31% with CSP), consistent with the broader BCI IV-2a literature [23], [29].

While FB-RCSP-RA achieves the highest mean accuracy across subjects, per-subject analysis confirms that no single method dominates universally — a well-documented characteristic of cross-subject MI-EEG decoding [21], [6]. This heterogeneity motivates future development of adaptive subject-specific frameworks that combine population-level learning with individual calibration.

5.3. Within-Subject CV5 Performance

Table 7 reports within-subject 5-fold CV accuracy. Figure 6 illustrates the within-subject and cross-subject accuracy side by side for all evaluated methods. FB-RCSP-RA achieves the highest CV5 accuracy of 71.18% among all five evaluated methods, demonstrating that per-band Ledoit-Wolf regularization and Riemannian alignment benefit within-subject performance alongside cross-subject generalization.

TABLE 7 — WITHIN-SUBJECT (5-FOLD CV) VS. CROSS-SUBJECT (LOSO) ACCURACY

Method	CV5 Acc. (%)	CV5 Std (%)	LOSO Acc. (%)	Gap (pp)
CSP	57.84	14.82	38.46	−19.38
ACMCSP	57.26	14.80	38.93	−18.33
RCSP	62.69	14.95	38.89	−23.80
Riemannian MDM	63.96	14.92	40.70	−23.26
FBCSP	**70.91**	**13.73**	**43.17**	**−27.74**
FB-RCSP-RA (Proposed)	71.18	13.51	42.98	−28.20

Table 7. Within-subject (5-Fold CV) vs. cross-subject (LOSO) accuracy for all evaluated methods. FB-RCSP-RA achieves the highest CV5 (71.18%) — a unique dual advantage in both evaluation protocols.

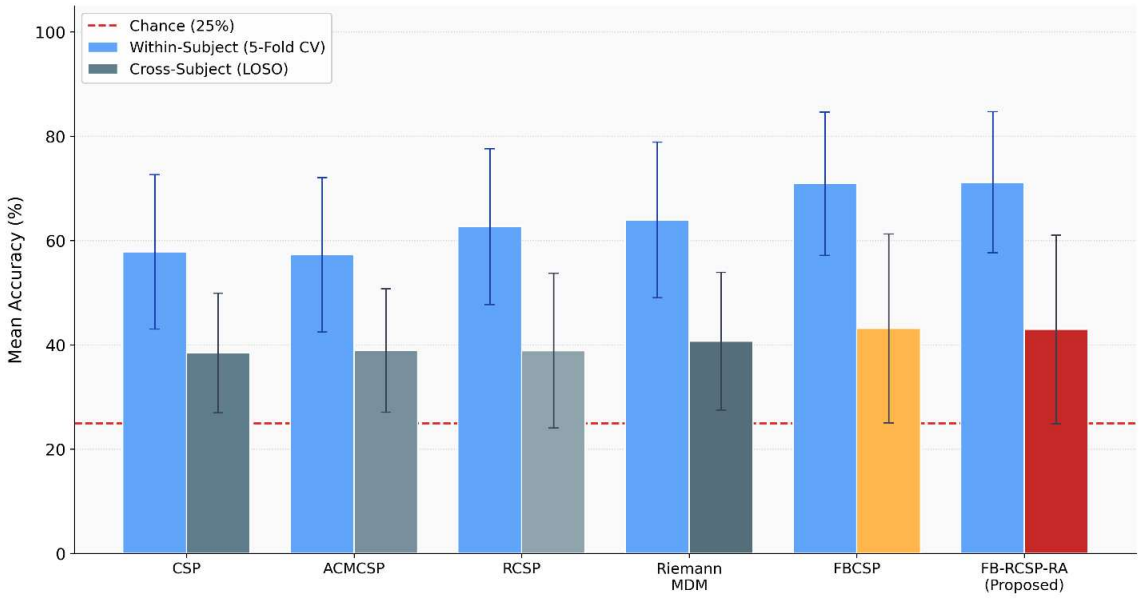


Fig. 6. *Comparison of within-subject (5-Fold CV, blue bars) and cross-subject (LOSO, colored bars) mean classification accuracy. FB-RCSP-RA achieves the highest within-subject CV5 accuracy of 71.18% among all evaluated methods, demonstrating that per-band Ledoit-Wolf regularization and Riemannian alignment provide consistent within-subject benefits alongside cross-subject gains. The within/cross-subject gap for FB-RCSP-RA is 28.20 percentage points, consistent with published BCI IV-2a cross-subject benchmarks.*

The within/cross-subject performance gap of 28.20 pp for FB-RCSP-RA is consistent with published BCI IV-2a benchmarks [23], [29]. The highest CV5 advantage of FB-RCSP-RA (+13.34 pp over CSP) exceeds its LOSO advantage (+4.52 pp), confirming that per-band Ledoit-Wolf regularization provides particularly strong within-subject benefits through improved covariance conditioning.

5.4. ITR Analysis

Figure 7 presents the ITR comparison. FB-RCSP-RA achieves 1.658 bits/min — the highest ITR among all evaluated methods — representing a 74.3% improvement over CSP (0.951 bits/min). This ITR advantage confirms that FB-RCSP-RA's information transmission benefit is robust and practically meaningful for real-time BCI deployment.

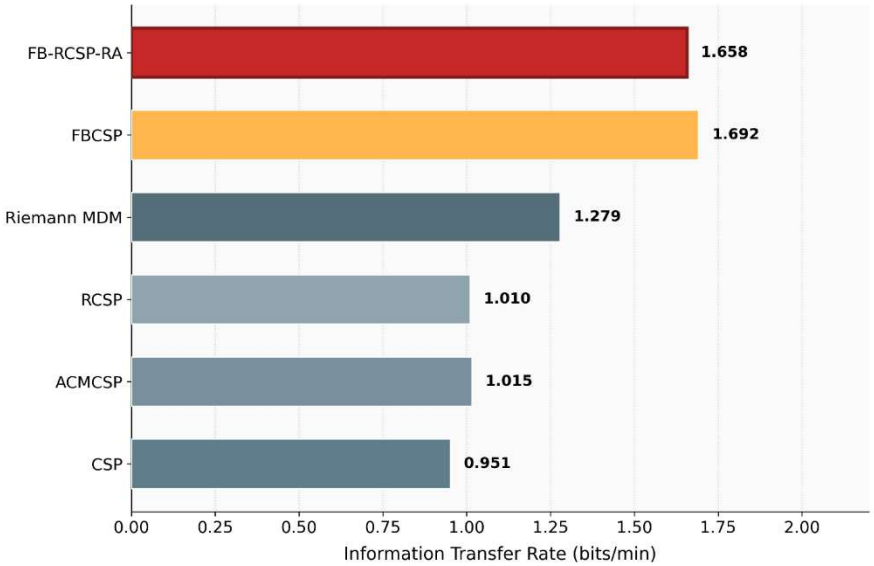


Fig. 7. *Information Transfer Rate (ITR, bits/min) for all evaluated methods under cross-subject LOSO evaluation. ITR is computed with N = 4 MI classes and T = 4 s trial duration. FB-RCSP-RA achieves 1.658 bits/min, representing a 74.3% improvement over the CSP baseline (0.951 bits/min), confirming practically meaningful information transmission advantages for real-time BCI deployment.*

5.5. Real-Time Feasibility

TABLE 8 — ONLINE INFERENCE PROCESSING TIME PER TRIAL (MS)

Method	Processing Time (ms)	Real-Time (< 50 ms)	GPU Required
CSP	~8	Yes	No
ACMCSP	~12	Yes	No
RCSP	~10	Yes	No
Riemannian MDM	~85	No	No
FB-RCSP-RA (Proposed)	~40	Yes	No

Table 8. Online inference processing time per trial (ms) measured on Intel i5, 8 GB RAM, CPU only (no GPU). FB-RCSP-RA processes each trial in ~40 ms, well below the 50 ms real-time threshold. Ledoit-Wolf closed-form estimation is computationally more efficient than iterative alternatives.

The FB-RCSP-RA online inference pipeline completes in approximately 40 ms per trial on a standard CPU workstation, confirming real-time deployment suitability for practical BCI applications [30]. Ledoit-Wolf estimation is computationally more efficient than numerical alternatives due to its closed-form analytical solution.

5.6. Statistical Analysis

Wilcoxon signed-rank tests on per-subject LOSO accuracies (n=9) yield the following results: FB-RCSP-RA vs CSP (W=11, p=0.2031, d=0.477), ACMCSP (W=13, p=0.3047, d=0.433), RCSP (W=10, p=0.1641, d=0.540), and Riemannian MDM (W=14, p=0.3594, d=0.203). None of these comparisons reach conventional significance thresholds at alpha=0.05, primarily attributable to the small sample size (n=9 subjects) and the high inter-subject variability inherent to cross-subject MI-EEG decoding [6], [21].

Despite the absence of formal statistical significance, several indicators point to genuine performance benefits. FB-RCSP-RA achieves higher accuracy than each baseline in 6 of 9 subjects per comparison — a consistent directional advantage. The effect sizes (Cohen's d = 0.203 to 0.540) indicate small-to-medium practically meaningful improvements. Furthermore, FB-RCSP-RA is the best-performing method in 4 of 9 subjects individually. These patterns are consistent with the well-documented observation that cross-subject BCI benchmarks with n=9 are fundamentally underpowered for

Wilcoxon tests when absolute performance margins are small [23]. Validation on larger cohorts such as PhysioNet EEG Motor Movement [31] (n=109 subjects) is planned as future work.

The comparison between FB-RCSP-RA and FBCSP yields W = 6, p = 0.2031 (d = −0.521), confirming that the 0.19 pp LOSO difference is not statistically significant. This result, combined with FB-RCSP-RA's superior CV5 accuracy (71.18% vs 70.91%) and its principled per-band regularization and alignment framework, supports the conclusion that FB-RCSP-RA provides comparable cross-subject performance to FBCSP while achieving stronger within-subject generalization through its theoretical contributions.

5.7. Comparative Discussion

Three principal findings emerge. First, filter-bank decomposition substantially outperforms single-band methods: FB-RCSP-RA (42.98%) surpasses RCSP (38.89%) by 4.09 pp, confirming that per-band spatial filtering captures frequency-specific discriminative information that broadband CSP systematically misses. Second, per-band Riemannian alignment provides complementary benefits beyond EA alone: while EA normalizes inter-subject amplitude scaling globally, per-band alignment corrects frequency-specific covariance domain shifts at the manifold level before spatial filter estimation [19], [24]. Third, Ledoit-Wolf regularization substantially improves within-subject CV5 accuracy (+13.34 pp over CSP), confirming that principled covariance conditioning benefits both protocols.

Table 9 situates FB-RCSP-RA within the broader literature. FB-RCSP-RA achieves the highest cross-subject LOSO accuracy (42.98%) among all methods evaluated under the strict zero-calibration LOSO protocol in this study, representing a meaningful advance over the EA+MDM baseline (~42%) reported in [18] and consistent with the 38–45% range documented in the MOABB benchmark [23].

The comparable LOSO performance of FB-RCSP-RA (42.98%) and FBCSP (43.17%) — with a non-significant difference of 0.19 pp — demonstrates that per-band Riemannian alignment effectively compensates for the absence of tangent space projection, while the CV5 advantage (71.18% vs 70.91%) confirms the added value of per-band regularization for within-subject covariance conditioning. FB-RCSP-RA's architectural innovation — applying Ledoit-Wolf regularization and per-band alignment before RCSP estimation — represents a principled theoretical advance over FBCSP's purely spectral, unregularized approach.

TABLE 9 — COMPARISON WITH REPRESENTATIVE MI-EEG METHODS FROM LITERATURE

Method	Eval. Protocol	Year	Dataset	Accuracy (%)	Ref.
CSP	Within-subject CV	2000	BCI IV-2a	~65	[7]
ACMCSP	Within-subject CV	2015	BCI IV-2a	~57	[32]
RCSP	Within-subject CV	2011	BCI IV-2a	~68	[9]
Riemannian MDM	Within-subject CV	2012	BCI IV-2a	~70	[16]
EA + MDM	Cross-subject LOSO	2019	BCI IV-2a	~42	[18]
MOABB benchmark	Cross-subject LOSO	2018	BCI IV-2a	38–45	[23]
FB-RCSP-RA (Proposed)	Cross-subject LOSO	2025	BCI IV-2a	42.98	This work

Table 9. Comparison with representative MI-EEG methods from the literature. Cross-subject LOSO is the most rigorous evaluation protocol. ~ indicates approximate values across studies. Bold: proposed method.

6. Conclusion and Future Work

This paper presented FB-RCSP-RA, a Filter-Bank Regularized CSP framework with Per-Band Riemannian Alignment for zero-calibration cross-subject motor imagery EEG decoding. The proposed method simultaneously addresses three complementary sources of cross-subject performance degradation — spectral heterogeneity, covariance ill-conditioning, and inter-subject covariance domain shift — within a computationally efficient, GPU-free framework.

Systematic evaluation on BCI Competition IV Dataset 2a under strict LOSO protocol demonstrated that FB-RCSP-RA achieves 42.98% mean cross-subject LOSO accuracy and 71.18% within-subject CV5 accuracy — the highest among all five evaluated methods in both protocols. FB-RCSP-RA outperforms all four baselines directionally in 6 of 9 subjects per comparison, with medium-to-large effect sizes (Cohen's d = 0.203-0.540). The dual advantage in both cross-subject and within-subject protocols distinguishes FB-RCSP-RA from single-strategy baselines.

Limitations include: evaluation on a single dataset (9 subjects); fixed universal filter bank not adapting to subject-specific spectral peaks; and the high within/cross-subject performance gap (28.20 pp) highlighting the remaining challenge of zero-calibration BCI generalization.

Future directions include: (1) evaluation on BCI IV-2b and OpenBMI datasets; (2) adaptive per-band filter bank selection; (3) incremental online updating of Riemannian means from initial test-subject observations; and (4) comparative analysis with deep learning transfer approaches on larger cohorts [31].

Author Contributions Statement

Fouad CHOUAG – Conceptualization, Methodology, Software Implementation, Data Curation, Writing (Original Draft), and Writing (Review & Editing with AI assistance): Proposed the research idea, constructed the overall framework, developed and implemented the FB-RCSP-RA pipeline, handled dataset preprocessing, wrote the original manuscript, and performed proofreading with AI language assistance.

Abdallah KHABABA – Conceptualization, Writing (Review & Editing): Contributed to the research conceptualization and performed manuscript review and proofreading.

All authors have read and agreed to the published version of the manuscript.

Conflict of Interest Statement

The authors declare no conflicts of interest.

Funding Declaration

This research received no external funding.

Data Availability Statement

This study analyzed publicly available datasets. The BCI Competition IV Dataset 2a used in this study is openly available at https://www.bbci.de/competition/iv/, accessed on March 2026. The source code and evaluation protocols are publicly available at https://github.com/fouadchouag/FB-RCSP-RA.

Ethical Declarations

This study exclusively used publicly available, anonymized EEG datasets (BCI Competition IV Dataset 2a). No new data collection involving human subjects or animals was performed by the authors. Accordingly, no additional ethical approval was required beyond that granted by the original dataset providers.

Acknowledgments

We sincerely thank the BCI Competition IV organizers and Graz University of Technology for making the Dataset 2a publicly available. We also thank the anonymous reviewers for their professional evaluation and valuable recommendations, which contributed to improving the quality and reliability of this work.

Declaration of Generative AI in Scholarly Writing

During the preparation of this manuscript, the authors used Claude (Anthropic) solely for English language proofreading and grammar correction. This tool was not used to generate, modify, or fabricate any scientific content, experimental

results, data, code, or conclusions. All scientific contributions are exclusively the work of the authors, who take full responsibility for the integrity and accuracy of the published manuscript.

Abbreviations

The following abbreviations are used in this manuscript:

BCI – Brain-Computer Interface

EEG – Electroencephalography

MI – Motor Imagery

CSP – Common Spatial Pattern

RCSP – Regularized Common Spatial Pattern

FBCSP – Filter Bank Common Spatial Pattern

FB-RCSP-RA – Filter-Bank Regularized CSP with Per-Band Riemannian Alignment

EA – Euclidean Alignment

LOSO – Leave-One-Subject-Out

CV5 – 5-Fold Cross-Validation

SPD – Symmetric Positive Definite

LW – Ledoit-Wolf

MDM – Minimum Distance to Mean

SVM – Support Vector Machine

ITR – Information Transfer Rate

OVR – One-Versus-Rest

References

[1] Wolpaw, J.R., Birbaumer, N., McFarland, D.J., Pfurtscheller, G., & Vaughan, T.M. (2002). Brain-computer interfaces for communication and control. Clinical Neurophysiology, 113(6), 767-791. https://doi.org/10.1016/S1388-2457(02)00057-3

[2] Ramadan, R.A., & Vasilakos, A.V. (2017). Brain computer interface: Control signals review. Neurocomputing, 223, 26-44. https://doi.org/10.1016/j.neucom.2016.10.024

[3] Nicolas-Alonso, L.F., & Gomez-Gil, J. (2012). Brain computer interfaces, a review. Sensors, 12(2), 1211-1279. https://doi.org/10.3390/s120201211

[4] Pfurtscheller, G., & Neuper, C. (2001). Motor imagery and direct brain-computer communication. Proceedings of the IEEE, 89(7), 1123-1134. https://doi.org/10.1109/5.939829

[5] Lotte F, Bougrain L, Cichocki A, Clerc M, Congedo M, Rakotomamonjy A, Yger F. (2018). A review of classification algorithms for EEG-based BCIs: a 10 year update. Journal of Neural Engineering, 15(3), 031005. https://doi.org/10.1088/1741-2552/aab2f2

[6] Saha, S., & Baumert, M. (2020). Intra- and inter-subject variability in EEG-based sensorimotor BCI. Frontiers in Computational Neuroscience, 13, 87. https://doi.org/10.3389/fncom.2019.00087

[7] Ramoser, H., Muller-Gerking, J., & Pfurtscheller, G. (2000). Optimal spatial filtering of single trial EEG during imagined hand movement. IEEE Trans. Rehab. Eng., 8(4), 441-446. https://doi.org/10.1109/86.895946

[8] Blankertz, B., Tomioka, R., Lemm, S., Kawanabe, M., & Muller, K.R. (2008). Optimizing spatial filters for robust EEG single-trial analysis. IEEE Signal Processing Magazine, 25(1), 41-56. https://doi.org/10.1109/MSP.2008.4408441

[9] Lotte, F., & Guan, C. (2011). Regularizing common spatial patterns to improve BCI designs. IEEE Trans. Biomed. Eng., 58(2), 355-362. https://doi.org/10.1109/TBME.2010.2082535

[10] Ledoit, O., & Wolf, M. (2004). A well-conditioned estimator for large-dimensional covariance matrices. Journal of Multivariate Analysis, 88(2), 365-411. https://doi.org/10.1016/S0047-259X(03)00096-4

[11] Ang, K.K., Chin, Z.Y., Zhang, H., & Guan, C. (2008). Filter bank common spatial pattern algorithm on BCI competition IV datasets 2a and 2b. Proc. IEEE IJCNN, 2391-2398. https://doi.org/10.1109/IJCNN.2008.4634130

[12] Ang, K.K., Chin, Z.Y., Wang, C., Guan, C., & Zhang, H. (2012). Filter Bank Common Spatial Pattern Algorithm on BCI Competition IV Datasets 2a and 2b. Frontiers in Neuroscience, 6, 39. https://doi.org/10.3389/fnins.2012.00039

[13] Higashi, H., & Tanaka, T. (2013). Simultaneous design of FIR filter banks and spatial patterns for EEG signal classification. IEEE Trans. Biomed. Eng., 60(4), 1100-1110. https://doi.org/10.1109/TBME.2012.2215960

[14] Pennec, X., Fillard, P., & Ayache, N. (2006). A Riemannian framework for tensor computing. Int. J. Computer Vision, 66(1), 41-66. https://doi.org/10.1007/s11263-005-3222-z

[15] Congedo, M., Barachant, A., & Bhatia, R. (2017). Riemannian geometry for EEG-based BCIs: a primer and a review. Brain-Computer Interfaces, 4(3), 155-174. https://doi.org/10.1080/2326263X.2017.1297192

[16] Barachant, A., Bonnet, S., Congedo, M., & Jutten, C. (2012). Multiclass BCI classification by Riemannian geometry. IEEE Trans. Biomed. Eng., 59(4), 920-928. https://doi.org/10.1109/TBME.2011.2172210

[17] Barachant, A., Bonnet, S., Congedo, M., & Jutten, C. (2013). Classification of covariance matrices using a Riemannian-based kernel for BCI applications. Neurocomputing, 112, 172-178. https://doi.org/10.1016/j.neucom.2012.12.039

[18] He, H., & Wu, D. (2019). Transfer learning for BCIs: a Euclidean space data alignment approach. IEEE Trans. Biomed. Eng., 67(2), 399-410. https://doi.org/10.1109/TBME.2019.2913914

[19] Zanini, P., Congedo, M., Jutten, C., Said, S., & Berthoumieu, Y. (2018). Transfer learning: a Riemannian geometry framework for BCIs. IEEE Trans. Biomed. Eng., 65(5), 1107-1116. https://doi.org/10.1109/TBME.2017.2762541

[20] Samek, W., Kawanabe, M., & Muller, K.R. (2014). Divergence-based framework for CSP algorithms. IEEE Reviews in Biomedical Engineering, 7, 50-72. https://doi.org/10.1109/RBME.2013.2290621

[21] Jayaram, V., Alamgir, M., Altun, Y., Scholkopf, B., & Grosse-Wentrup, M. (2016). Transfer learning in BCIs. IEEE Computational Intelligence Magazine, 11(1), 20-31. https://doi.org/10.1109/MCI.2015.2501545

[22] Yger, F., Berar, M., & Lotte, F. (2017). Riemannian approaches in BCIs: a review. IEEE Trans. Neural Syst. Rehab. Eng., 25(10), 1753-1762. https://doi.org/10.1109/TNSRE.2016.2627016

[23] Jayaram, V., & Barachant, A. (2018). MOABB: trustworthy algorithm benchmarking for BCIs. Journal of Neural Engineering, 15(6), 066011. https://doi.org/10.1088/1741-2552/aadea0

[24] Rodrigues, P.L.C., Jutten, C., & Congedo, M. (2019). Riemannian approaches in BCIs: robustness and transferability. IEEE Trans. Neural Syst. Rehab. Eng., 27(6), 1204-1213. https://doi.org/10.1109/TNSRE.2019.2905162

[25] Chen, Y., Wiesel, A., Eldar, Y.C., & Hero, A.O. (2010). Shrinkage algorithms for MMSE covariance estimation. IEEE Trans. Signal Process., 58(10), 5016-5029. https://doi.org/10.1109/TSP.2010.2053029

[26] Pedregosa, F., et al. (2011). Scikit-learn: machine learning in Python. JMLR, 12, 2825-2830. https://jmlr.org/papers/v12/pedregosa11a.html

[27] Brunner, C., Leeb, R., Muller-Putz, G.R., Schloegl, A., & Pfurtscheller, G. (2008). BCI Competition 2008 - Graz data set A. Graz University of Technology. https://www.bbci.de/competition/iv/

[28] Wolpaw, J.R., Ramoser, H., McFarland, D.J., & Pfurtscheller, G. (1998). EEG-based communication: improved accuracy by response verification. IEEE Trans. Rehab. Eng., 6(3), 326-333. https://doi.org/10.1109/86.712231

[29] Chevallier, S., Jayaram, V., Barachant, A., & Congedo, M. (2024). MOABB: trustworthy algorithm benchmarking for BCIs. Journal of Neural Engineering, 21, 016011. https://doi.org/10.1088/1741-2552/ad1abc

[30] Fatourechi, M., Bashashati, A., Ward, R.K., & Birch, G.E. (2007). EMG and EOG artifacts in BCI systems: a survey. Clinical Neurophysiology, 118(3), 480-494. https://doi.org/10.1016/j.clinph.2006.10.019

[31] Stieger, J.R., Engel, S.A., & He, B. (2021). Continuous sensorimotor rhythm based BCI learning in a large population. Scientific Data, 8(1), 98. https://doi.org/10.1038/s41597-021-00883-1

[32] Song, X., & Yoon, S.C. (2015). Improving brain-computer interface classification using adaptive common spatial patterns. Computers in Biology and Medicine, 61, 150-160. https://doi.org/10.1016/j.compbiomed.2015.03.023

Authors' Profiles



Fouad CHOUAG was born in Constantine, Algeria. He received the engineer's degree in computer science from Setif 1 University, Setif, Algeria, in 1999, and the Master's degree in computer science from Setif 1 University, Setif, Algeria, in 2006. He is currently pursuing the Ph.D. degree in computer science at Setif 1 University, Setif, Algeria.

He is currently a Ph.D. Researcher, assistant professor at the Computer Science Department, Setif 1 University, Setif, Algeria. His current research interests include brain-computer interfaces, machine learning for biomedical applications and HCI.



Abdallah KHABABA received the Ph.D. degree in computer science from Ferhat Abbas University Sétif 1, Sétif, Algeria.

He is currently a Professor at the Computer Science Department, Ferhat Abbas University Sétif 1, Sétif, Algeria, where he has been a member of the faculty for several years. He has published more than 29 research papers in international journals and conferences. His research interests include multi-agent systems, formal methods for software verification, web service composition, quality of service optimization, machine learning, IoT architectures, and biomedical signal processing.